A Novel Design of a Desiccant Rotary Wheel for Passive Ventilation Applications

Dominic O'Connor*[1], John Kaiser Calautit[1], Ben Richard Hughes[1]

[1]Department of Mechanical Engineering, University of Sheffield, Sheffield S10 2TN, UK

*Corresponding author: dboconnor1@sheffield.ac.uk

Abstract

Rotary desiccant wheels are used to regulate the relative humidity of airstreams. These are commonly integrated into Heating, Ventilation and Air-Conditioning units to reduce the relative humidity of incoming ventilation air. To maximise the surface area, desiccant materials are arranged in a honeycomb matrix structure which results in a high pressure drop across the device requiring fans and blowers to provide adequate ventilation. This restricts the use of rotary desiccant wheels to mechanical ventilation systems. Passive ventilation systems are able to deliver adequate ventilation air but cannot control the humidity of the incoming air. To overcome this, the traditional honeycomb matrix structure of rotary desiccant wheels was redesigned to maintain a pressure drop value below 2Pa, which is required for passive ventilation purposes. In addition to this, the temperature of the regeneration air for desorption was lowered. Radial blades extending out from the centre of a wheel to the circumference were coated in silica gel particles to form a rotary desiccant wheel. Computational Fluid Dynamics (CFD) modelling of the design was validated using experimental data. Reduction in relative humidity up to 55% was seen from the system whilst maintaining a low pressure drop across the new design. As an outcome of the work presented in this paper, a UK patent GB1506768.9 has been accepted.

Keywords: Rotary desiccant wheel; Passive ventilation; Computational Fluid Dynamics; Dehumidification; Rapid Prototyping; Wind Tunnel

Introduction

Up to 80% of a person's time is now spent indoors in a closed environment [1]. This means that the indoor conditions to which occupants are subject to must conform to occupant demands, and should be managed by systems capable of delivering these demands. Thermal comfort, good air quality to maintain health, reliability and control of the system are all key to delivering satisfactory internal conditions for occupants [2]. At present, this role is primarily fulfilled by mechanical Heating, Ventilation and Air-Conditioning (HVAC) systems. Whilst mechanical HVAC systems are capable of delivering the necessary conditions to occupants of comfortable indoor conditions, high energy consumption of such systems contributes a significant amount of greenhouse gas emissions to the climate. The construction, operation and maintenance of buildings accounts for 40% of the total global energy consumption [3]. Within this sector, HVAC systems account up to 40% of the total consumption [4]. Reducing the energy consumption of HVAC systems would substantially reduce the energy consumption of buildings and lead to a reduction in greenhouse gas emissions [5].

The relative humidity of incoming supply air can have a significant impact on the energy consumption of HVAC systems [6]. High relative humidity levels coupled with moderate-to-high air temperature leads to discomfort to occupants, this is caused by high moisture levels in the air

preventing evaporation of sweat from the skin's surface [7]. As sweat cannot evaporate, the body's natural cooling mechanism cannot operate effectively and so body temperature rises, increasing the thermal discomfort felt by the occupant. By reducing the level of relative humidity in the air, occupant comfort would increase. High moisture content of indoor air can also have serious health implications for occupants. The presence of high moisture content and warm indoor air temperatures can result in the growth of bacteria and mould [8]. The spores emitted from these growths can affect occupant health, primarily relating to respiratory and skin problems [9]. Reducing the relative humidity of indoor air and maintaining continuous ventilations prevents bacteria and mould build-up.

Rotary desiccant wheels are energy recovery heat exchangers that operate with regard to relative humidity reduction and are often utilised in mechanical air-conditioning systems. The walls of the rotary wheel are commonly fabricated in a honeycomb or sinusoidal shape to form a matrix structure to maximise the surface area, this can be seen in Figure 1.

Figure 1 –Section of the matrix of a desiccant wheel for mechanical HVAC

In this application, desiccant materials are used to transfer moisture from one airstream to another through the process of adsorption and desorption [10]. The mechanisms of adsorption and desorption in desiccant materials have been thoroughly explored in literature [11] along with the various desiccant materials which can be used in rotary desiccant wheel systems [12][13]. Desiccant materials have moisture adsorptive properties; the adhesion of gas, liquid or dissolved solids molecules to the surface of a solid. Adsorption is a weak interaction and can be reversed. In the case of desiccant rotary wheels used for ventilation, silica gel (hydrated silicon dioxide) is the most common desiccant material used for a wide range of applications [14].

There are a number of factors which restrict the widespread uptake of these recovery devices. A high pressure drop in the air flow is experienced across devices, typically up to 100Pa depending on the system type and configuration [15]. This can be overcome in mechanical systems with fans and blowers. Furthermore, the temperature required for desorption of the water from the surface of the desiccant is generally within the range of 80-120°C which incurs high energy costs from the regeneration airstream. For desiccant rotary wheels to become a more commonly integrated device in ventilation systems, modifications to the systems are required which can alter the incoming air to maximise comfort to occupants, exhibit low pressure drop on the air flow and operate continually and successfully with a lower regeneration temperature.

Rotary desiccant wheels operate by continuously rotating between two or more airstreams at a low angular velocity. The airstreams have varying conditions; for example in a temperate climate such as the UK, the inlet airstream is cooler with high relative humidity whereas the exhaust/regeneration airstream is drier with a higher air temperature. The section of the wheel which is rotating through an airstream with high relative humidity adsorbs moisture onto the desiccant. The process of adsorption results in a temperature increase of the humid airstream, in certain climates this requires the air to be cooled for thermal comfort. This two-step approach can incur significant additional cost if systems are inappropriately designed. The continued rotation of the wheel results in the section of the wheel which is saturated moving into the drier, hotter airstream. Here, desorption takes place where the moisture on the surface of the desiccant is released into the airstream due to the high temperature and low relative humidity, where the silica gel returns to its original state before adsorption.

A new, and previously untested, structure for rotary desiccant wheels was conceptualised, designed and tested to achieve these aims. By replacing the traditional honeycomb/sinusoidal wave matrix structure of the desiccant wheel with blades which extend out from the centre of the wheel, it was envisioned that a high levels of moisture adsorption could be achieved. Further aims of the redesigned desiccant wheel were to lower the regeneration temperature and pressure drop across the wheel due to the large openings between the blades, when compared to existing devices. The new design of the rotary desiccant wheel, termed as the “radial blade design”, was analysed using experimental testing to validate computational fluid dynamics (CFD) models for the same geometry. 3D prototyping was carried out to build the desiccant rotary wheel used to validate the CFD models. No previous work has been conducted redesigning the structure of the desiccant wheel matrix to reduce relative humidity levels and limit the pressure drop, enabling integration into a wind tower or other passive ventilation system.

Previous Related Work

The rate at which the desiccant material adsorbs/desorbs moisture can be controlled by building operators and so can regulate the relative humidity of the incoming air as conditions dictate [16]. Factors include the type of desiccant used, the amount of desiccant used, and the rotation speed of the wheel, the depth of the wheel and the structure of the matrix [17]. Though maximising the amount of desiccant within the rotary desiccant wheel leads to maximum moisture transfer; the structural design and depth of the matrix results in a high pressure drop in the airstream [18]. The high pressure drop in the incoming airflow results in inadequate ventilation rates to the building. Additional high powered fans are installed in mechanical HVAC systems to overcome the high pressure drop and provide suitable ventilation air [19]. However, the additional energy demand from the high powered fans lead to increased energy consumption for the system as a whole. Though the relative humidity of the incoming air is maintained at required levels for the occupants, the increased energy consumption and cost requires evaluation [20]. Recent work has shown that though the energy costs exist for energy consumption in these systems, a hybrid desiccant cooling system, when compared to other air-conditioning systems, was effective at reducing energy demands. However, the current initial capital costs are not offset the savings and so further investigation is required [21].

The regeneration temperature, the temperature to which the exhaust air is raised to is another process which requires high energy demand for successful operation of the system. The typical

regeneration air temperature required for desorption of the silica gel takes place can be as high as 120°C [22]. This further increases the high energy demand for the system as a whole. Attempts have shown that lower regeneration temperatures are capable of maintaining desorption of the silica gel [23]. It is important that desorption is maintained, allowing the silica gel to continue to adsorb the moisture from the inlet air and improving comfort, if the desorption process is interrupted, the silica gel may become completely saturated and no longer be capable of reducing the relative humidity of the airstream by adsorption.

Reducing the regeneration air temperature as low as possible will result in lower overall energy consumption and increase the attractiveness of the systems to building operators [24]. Other research shows that desorption at lower regeneration temperatures may be possible when the velocity of the inlet and regeneration air are controlled for optimum desorption [25]. Other sources for regeneration heat have been explored, using solar energy in parabolic concentrators to increase air temperature has shown positive results when coupled with a new system of desiccant dehumidification [26].

In order to provide thermal comfort to occupants for a range of outdoor conditions with low energy requirements, less conventional systems should be explored. Wind towers are a passive ventilation system that are able to provide adequate ventilation air to a building with zero energy input [27]. By manipulating the principles of pressure driven flow in the forms of wind flow and the stack (buoyancy) effect, wind towers are more effective at providing ventilation than solely relying on windows and openings [28]. Wind towers are becoming increasingly more common as ventilation solutions in high occupant density buildings such as schools and commercial office spaces [29] and have shown that along with the benefit of reducing the reliance on mechanical HVAC and reducing energy consumption [30], wind towers provide fresh, clean outdoor air whilst extracting contaminated air, improving the cognitive performance of occupants and providing a healthier environment [31].

Despite the benefits of passive ventilation systems providing fresh, clean air whilst reducing energy consumption, there are limitations to the operational window of wind towers [32]. In temperate climates where the uptake of wind towers has been high, the operational window of wind towers is limited by the external climate conditions. As wind towers ventilate by introducing outdoor air directly into the occupied spaces, if the temperature of the external air falls outside the comfortable range of conditions, the dampers are closed to prevent any outdoor air being introduced. The UK Workplace (Health, Safety and Welfare) Regulations 1992 [33] sets a legal obligation on employers and building managers to provide a working environment that is suitable for employees. The advised temperature from the Approved Code of Practice is 16°C for the majority of working environments, but can be lower for spaces where significant manual effort is conducted. When outdoor air temperatures fall below 16°C, the operation of wind towers is not suitable. Equally, if the outdoor air temperature rises above indoor air temperatures, commonly between 20-22°C, the introduction of this air without conditioning will create discomfort for the occupants. This also applies to indoor humidity level which ideally should be between 40-60%, a figure endorsed by HEVAC, CIBSE, BSRIA and *BR.*

Integrating complimentary technologies into the ductwork below a wind tower which are capable of modifying the incoming air, either through heating, cooling or drying, would be greatly beneficial to

building operators by increasing the operational window of wind towers. Examples of attempts to couple these systems have been seen previously. Capturing heat from exhaust air and transferring it to the incoming air would raise the temperature. This concept would reduce the energy required for heating whilst providing clean air, various designs have been attempted and explored by a number of research teams with different heat recovery devices [34,35]. As cooling of the incoming air is required in hot climates, the installation of devices and techniques to reduce the incoming air temperature have been attempted. These attempts include the use of heat pipes, evaporative cooling, and thermal mass buildings among other designs [36,37]. High relative humidity levels, which also affect thermal comfort of occupants, can be reduced by using desiccant systems, of which there are a number of configurations[38–40]. Desiccant systems generally require coupling to a cooling device also as the process of moisture removal increases air temperature, this leads to a further pressure drop along with the high pressure drop of desiccant systems.

A major restriction integrating recovery devices into a wind tower is the high pressure drop experienced across devices. Due to the low air velocity of incoming air in wind towers, a pressure drop across a device 2Pa or above results in negligible supply air. Recovery devices have significantly higher pressure drop, up to 100Pa. Though this is overcome in mechanical systems with fans and blowers, the additional energy required for this configuration is seen as unsatisfactory and surplus for a passive ventilation system. In order to extend the operational window of wind towers and maintain the low energy consumption demands, modifications to the systems are required which can alter the incoming air to maximise comfort to occupants. Devices which exhibit low pressure drop and are able to condition the air to a suitable level are required. Therefore this work will address the current research gap by investigating the potential of integrating a new design of rotary desiccant wheel into passive ventilation and ensuring that the system can supply the required fresh air rates while maintaining the dehumidification performance. A conceptual design of this can be seen in Figure 2.

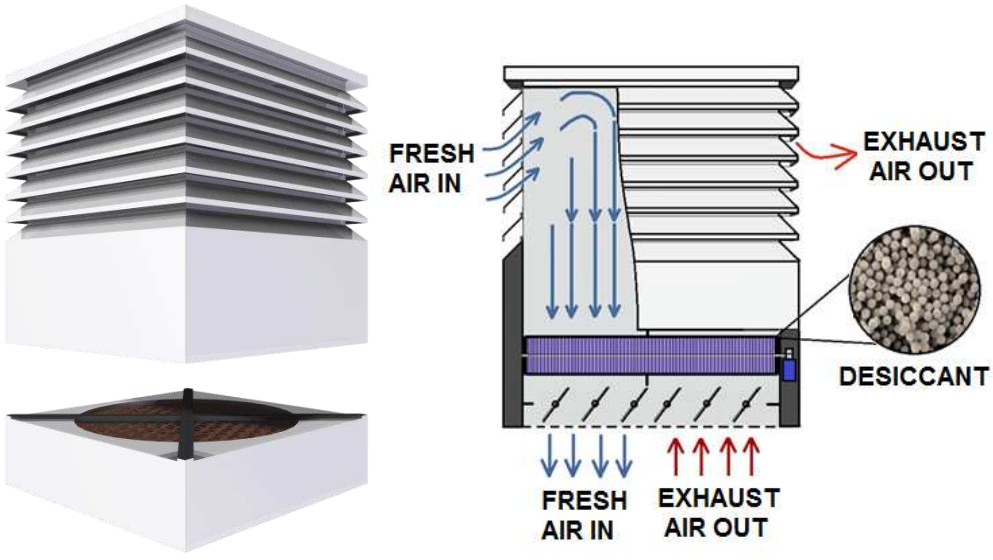

Figure 2 – Wind tower with desiccant rotary wheel integration concept

Novel Design of a Rotary Desiccant Wheel

Current desiccant rotary wheels use tightly packed matrices for moisture transport which can yield high efficiency. Though efficient, these matrices create a high pressure drop as air passes through.

This necessitates the use of high powered fans to force the required air through the wheel for ventilation which can further increase the energy requirements. Instead of a honeycomb structure, radial plates coated with desiccant silica gel particles, see Figure 3, and were inserted into a rotary wheel.

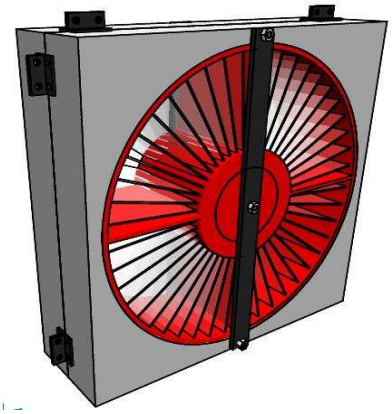

Figure 3 – 3D CAD model of the radial blade rotary desiccant wheel design

The geometry of the radial blades design was limited by the constraints of the equipment used for the construction of the experimental design. The external wheel diameter was 300mm with a depth of 105mm. An inner diameter of 40mm was made to allow a shaft to be inserted about which the wheel could rotate. Silica gel beads, approximately 1mm in diameter, were applied to the faces of 1mm thick acrylic plastic sheets with dimensions of 100x100mm. These formed the desiccant structure of the radial blade design. 28 blades were inserted into the wheel shell, this can be seen in Figure 4. The porosity of the design is 66.1%. This is significantly lower than the usual 90% porosity for honeycomb and sinusoidal wave structure rotary wheels [41]. However, it was expected that the greater individual volumes between the blades would ensure that the pressure drop did not exceed the aim of 2Pa. 3D printing was used to create the full rotary desiccant wheel design except for the silica gel and its plates and the motor.

A

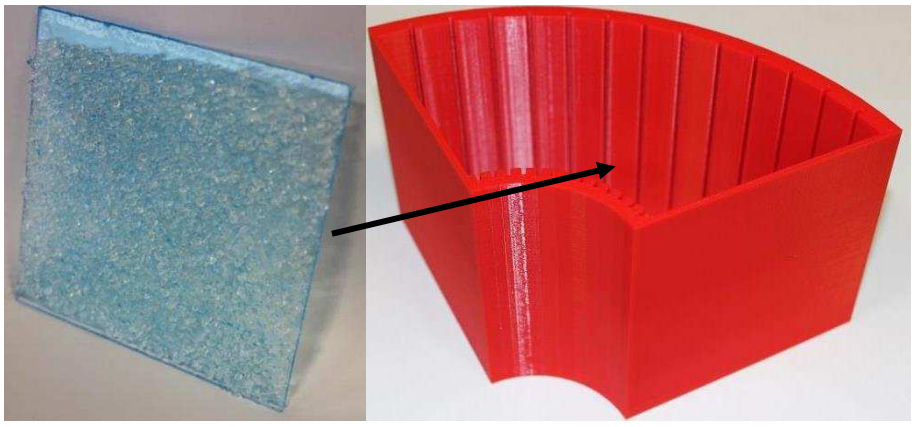

B

Figure 4 (a) Silica gel granules applied to Perspex sheets for insertion into wheel (b) Section of 3D printed desiccant rotary wheel with grooves for silica gel plates

As two separate air flows with different conditions were required for testing, a custom ductwork was built from acrylic sheeting. Two adjacent channels were constructed of equal length and which prevented any crossover of the airstreams. Seals were used between the gaps of the wheel and duct work to minimise crossover of the airstreams. The duct work was 500mm in length in both flow

directions from the rotary desiccant wheel and 325x325mm square in profile. The flow of the air was designed for counter-current flow to reflect the operation of a two or four-sided wind tower where the incoming air would be moving in the opposite direction to the exhaust air.

Experimental Setup

In order to assess the adsorption/desorption and pressure drop properties of the rotary desiccant wheel, experimental testing was conducted on a prototype rotary desiccant wheel which was subject to two independent cross-flow airstreams with different conditions. The components which made up the wheel were produced from the CAD models shown above using a 3D printer. This ensured the components were precisely manufactured. The flow through the ductwork was controlled by four 150mm diameter axial air fans (airflow speed up to 298m^3/hour), two mounted at each end of the ductwork. The air velocity through the ductwork was controlled by the fans which could be varied according to the requirements of the experiment. Mesh cloths were put over the opening of each of the air channels for straightening the flow to improve the uniformity of the air flow through the channels. The full experiment setup can be seen in Figure 5.

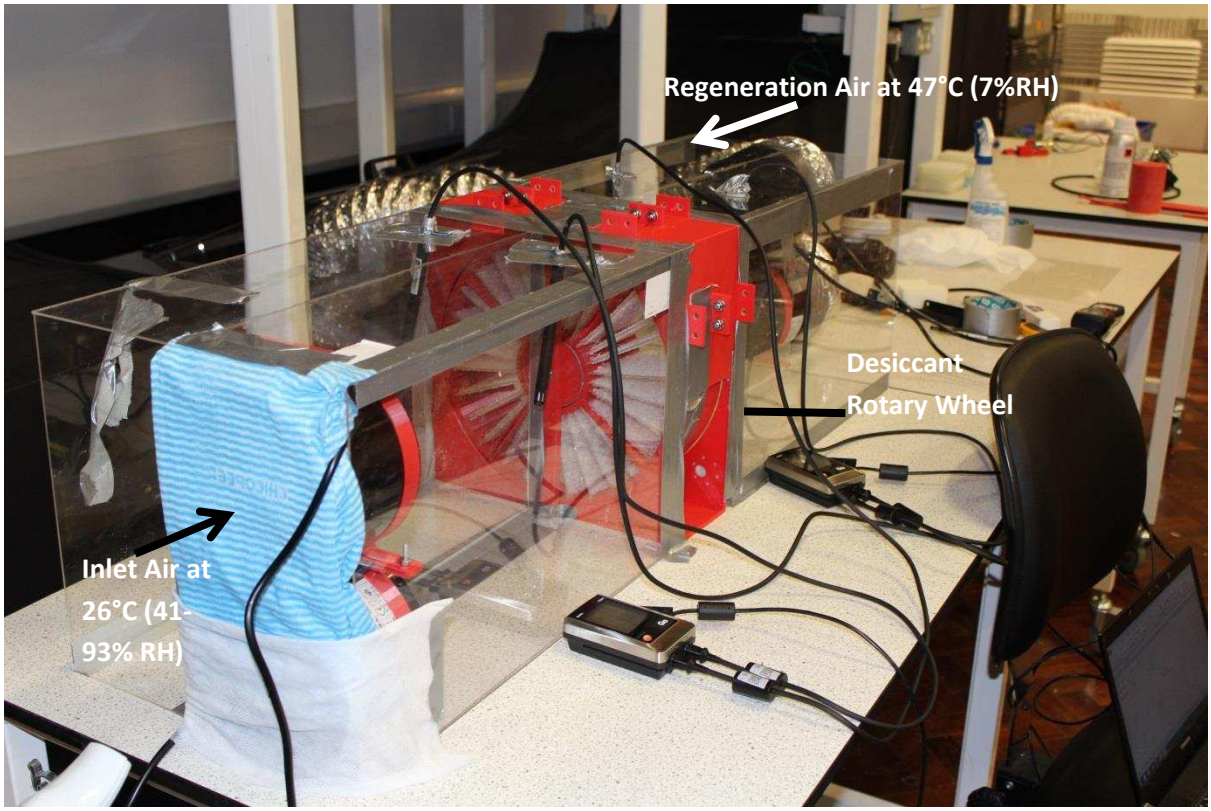

Figure 5 – Experimental Setup of Desiccant Rotary Wheel

Different properties were required for each of the air channels to assess the characteristics of the rotary desiccant wheel, and so different inputs were required for each airstream. As the regeneration air is required to be at a higher temperature and low relative humidity; air fed in from a closed circuit wind tunnel with a heater through a 150mm diameter flexible duct was used. The temperature of the air within the wind tunnel was set to the maximum value attainable by the wind tunnel heater, 55°C. This translated to a regeneration air temperature of 48°C in the rotary wheel ductwork. This is significantly lower than the regeneration temperature normally associated with desiccant rotary wheels. It was assumed that the large particle size of the silica gel would encourage

desorption at lower regeneration temperatures. The air within the closed loop wind tunnel was dry due to the closed circuit and continuous heating the heater. Further details of the wind tunnel can be found in [42]. The inlet air was required to be cooler with a high relative humidity. The ambient air of the laboratory was measured as 26°C and was determined to be suitable. The ambient relative humidity of the laboratory air was approximately 41%. This was increased by using a humidifier, directing water vapour onto the mesh cloths used to provide uniformity to the air flow. This increased the relative humidity inside the channel to a maximum of 93%. The increase in relative humidity reduced the air temperature to 20°C due to the evaporative cooling effect. The full properties of the experiment can be seen in Table 1.

Table 1 Properties of air channels and experiment

Input Condition	**Value**
Inlet Air Velocity	0.8m/s
Inlet Air Temperature	20-26℃ (293-300K)
Inlet Air RH	41-93%
Regeneration Air Velocity	0.8m/s
Regeneration Air Temperature	48℃ (321K)
Regeneration Air RH	7%
Rotation Speed	1.5-2rpm
Desiccant Material	Silica Gel
No. of Plates	28

Measurements of relative humidity and air temperature were simultaneously taken at four points before and after the desiccant rotary wheel in both the inlet and regeneration air channels. The measurement points were located 150mm from the surface of the wheel in the channel direction at the channel mid-height. Testo Humidity/Temperature probes, with accuracy of ±0.3°C temperature and ±2% relative humidity and range 2-98% relative humidity, were used for the measurements of the channel air. The values of relative humidity and air temperature were logged every second for ten minutes. The data was stored in two Testo 176P1 Data Loggers, capable of dual channel inputs and recording both relative humidity and temperature for two measurement points. For the first minute of testing the humidity generator was not directed down the inlet air channel in order for a clear differentiation to be seen between active adsorption and standard operation. The wheel was rotated continually for the entire test period.

CFD Methodology

The general purpose, commercial CFD code ANSYS FLUENT 15 was used to recreate the conditions of the experiment and simulate the airflow, relative humidity and temperature through the ductwork. A number of simulations were completed which were conducted with steady-state conditions in three dimensional space. The Finite Volume Method (FVM) with the Semi Implicit Method for Pressure Linked Equations (SIMPLE) velocity-pressure coupling algorithm was used. The k-ε turbulence model with standard wall functions was used to simulate the turbulent nature of the airflow [43]. The governing equations of this turbulence model have not been modified and so are not shown here but can be found elsewhere in literature [44].

The geometry created in SOLIDWORKS CAD software used to build the experiment prototype, including the ductwork, was used for the generation of the CFD models. This guaranteed that the dimensions of the two methods of analysis were identical. The explicit geometric modelling of the

physical design meant it was unnecessary to apply porous zone settings to the simulation to represent the passive desiccant rotary wheel. Alteration of the geometry would require recalculation of the coefficients used for the porous jump settings and validation for accuracy; physically modelling the geometry negates this requirement. The silica gel was modeled with two different approaches to represent the two aspects of it properties. The physical geometry of the silica gel applied to the plates was modelled as a solid, increasing the width of the radial plates to 3mm. This helped to maintain the accuracy of the geometry between the experimental model and the CFD model. The silica was also modelled as a fluid volume within the space between radial blades, this can be seen in Figure 6. Because the silica was modeled as a fluid, the air flow moved through it unimpeded and the volumes did not interfere with the velocity and pressure of the air through the radial blades. Additional settings, explained below, were added to the fluid silica volumes to represent the adsorption and desorption characteristics of the silica gel on the air.

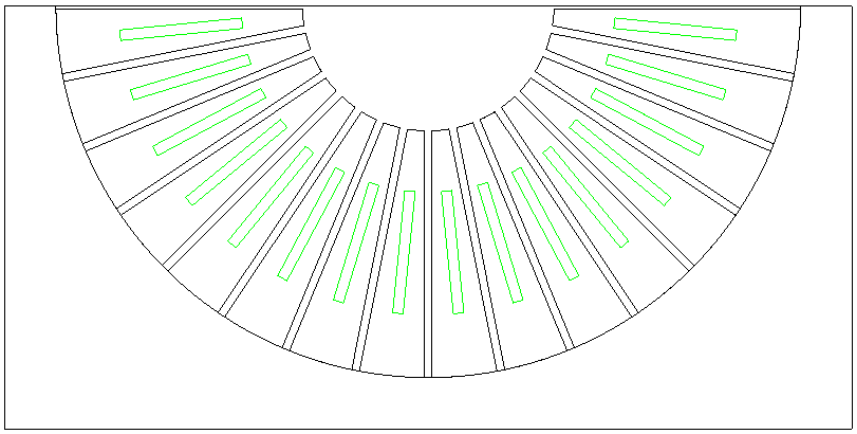

Figure 6 – Geometry of single duct with desiccant rotary wheel. Silica gel volume shown in green.

Grid Independency

The CAD geometry was imported into ANSYS DesignModeller to generate the computational models for CFD analysis. Due to the simple geometry of the rotary desiccant wheel and ductwork, a structured mesh was used for the surface and volumes of the computational domains. The number of cells used for meshing was between 6,800 and 920,000 cells, verification of the meshes was obtained by using the h-p adaption method to find accurate results, balanced by fast computational time. A consistent point was chosen to measure the temperature at for each mesh, the changes of this measured temperature were then compared, as seen in Figure 7. The final mesh used was 420,000 elements.

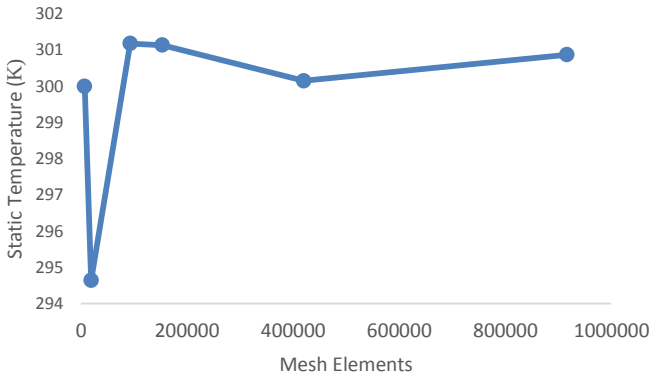

Figure 7 – h-p grid adaption of mesh used for CFD simulation

Boundary Conditions

Boundary conditions which replicate the conditions experienced in the experiment are required for the accurate simulation of flow. Using the appropriate configurations and values is essential in conducting a simulation that is as close to the conditions seen in the experiment. Two sets of inflow boundary conditions were required, one to simulate the airflow in the inlet channel airstream and one for the airflow of the regeneration channel airstream. The model used for the simulation of the airflow required two velocity inlets and two pressure (atmospheric) outlets. Vertical surfaces at each of the ductwork openings were used as inlet and outlets. Each velocity inlet was positioned opposite a pressure outlet along the same channel. As the two flows were moving counter-current, the velocity inlets were positioned at each end of the ductwork. The remaining surfaces were characterised as wall surfaces. The velocity, air temperature and mass fraction of H_2O, used to simulate the relative humidity, were set for the velocity inlet boundaries. The air velocity was maintained at each inlet but the mass fraction of H_2O and air temperature were altered to reflect the relative humidity and air temperature in the channel for inlet/regeneration air. These conditions can be seen in Table 2 below. The rotation of the rotary desiccant wheel was controlled with the reference frame control. A rotation speed of 2rpm was set for the wheel. Measurement points were plotted within the CFD model to match the measurement points of the experiment to ensure accuracy.

Table 2 – CFD Model Boundary Conditions for Adsorption/Desorption Profiles

Input Condition	**Value**	
	Inlet Air	**Regeneration Air**
Air Velocity	0.8m/s	0.8m/s
Air Temperature	293K	321K
H_2O Mass Fraction of Air	0.013g/g	0.005g/g
Rotation Speed	2rpm	2rpm
Energy Source/Sink	750000w/m^3	-250000w/m^3
Mass Source/Sink	-0.6kg/m^{3}s	0.2kg/m^{3}s
H_2O Source/Sink	-0.6kg/m^{3}s	0.2kg/m^{3}s

The simulation modelled volumes of silica gel used in the rotary desiccant wheel and ductwork. As the geometry of the experiment was symmetrical, and for time and computational efficiency, it was decided to model only a single channel at a time. The boundary conditions and simulation settings of the solver were altered to independently represent adsorption and desorption. Source term functions were applied to cell zone conditions in FLUENT to represent adsorption and desorption of

the silica gel. The material properties of silica gel were applied to the fluid volume, using sink/source (s/s) terms for adsorption/desorption (a/d) respectively. S/s terms are used to add and remove characteristics of the fluid flow, such as energy, mass, species and momentum, at a predetermined rate. Energy, mass and species terms are required for a/d and were set for the characteristics of the silica gel. The solver requires the same s/s values for mass and species to be set as inputs to ensure calculation stability. Energy s/s terms are used for the increase or decrease in dry bulb temperature, the change in temperature occurring as a result of a/d processes. The values for the s/s terms can be seen above in Table 2.

Validation of CFD Model

Comparison of the values measured in the experiment and the values measured from the CFD models is necessary for validation of the CFD models to confirm their accuracy and reliability for future modelling. Values of air temperature and relative humidity were measured from the CFD simulations at the same position as the experiment for accuracy.

Table 3 shows the comparison between values calculated from the CFD simulations and the measurements taken from the 600 second time step of the experiment. The error between the CFD results and the experimental data is included for comparison and validation.

Table 3 – Comparison and Validation of CFD model using Experimental Results

		TEMPERATURE (°C)		RELATIVE HUMIDITY (%)	
		Before Wheel	After Wheel	Before Wheel	After Wheel
ADSORPTION	CFD	20.00	27.14	90.70	33.14
	Experiment	20.11	27.46	91.28	27.46
	Error %	**0.55**	**1.17**	**0.64**	**-20.68**
DESORPTION	CFD	48.00	45.54	7.32	11.45
	Experiment	49.68	45.29	6.60	10.23
	Error %	**3.38**	**-0.55**	**-10.91**	**-11.93**

The error between the CFD and experiment data for the temperature readings is lower than the relative humidity readings. As the air temperature for the inlet boundary conditions can be set precisely, this is not unexpected for the readings before the wheel. The low error between the temperature readings for both the adsorption and desorption cases after the wheel however show greater accuracy and reliability between the two methodologies. Higher errors are introduced for the relative humidity readings for both cases with the CFD simulations consistently overestimating the relative humidity when compared to the experimental data. However, the degree to which the error is increased is notable due to the lower initial values of the data. As the values are small, differences of 0.72rH% and 1.22rH% between the two readings are more pronounced when computed as a percentage of the total value. The CFD models provide a credible method of analysing the new design of desiccant wheel which could be further improved by refinement of the boundary conditions and solver settings.

Results and Discussion

Air temperature and Relative Humidity

Figure 8 and Figure 9 show the CFD contours of temperature and relative humidity of the inlet and regeneration channels of the duct and desiccant rotary wheel respectively. The values from the CFD measurement can be seen in Table 3 and compared with the measurements from the experiment.

Good agreement between the experiment values and CFD values were seen for both the air temperature and relative humidity.

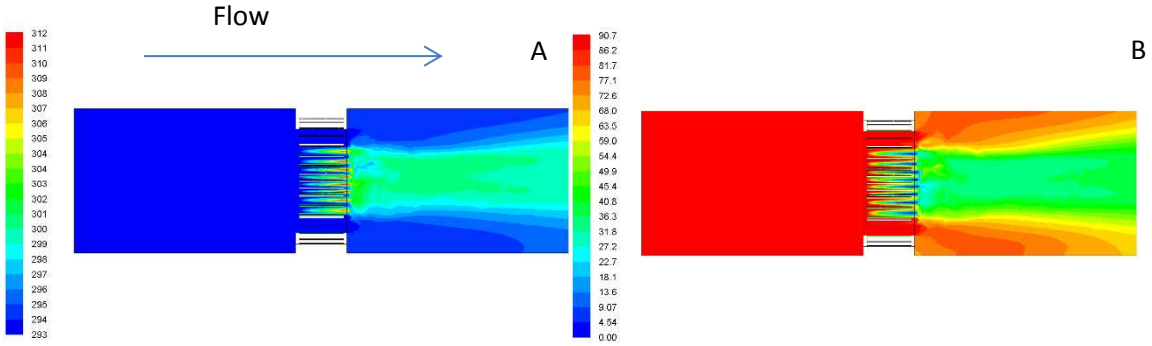

Figure 8 – Contours of a) temperature (in K) and b) relative humidity (%) for the CFD model of the inlet air channel

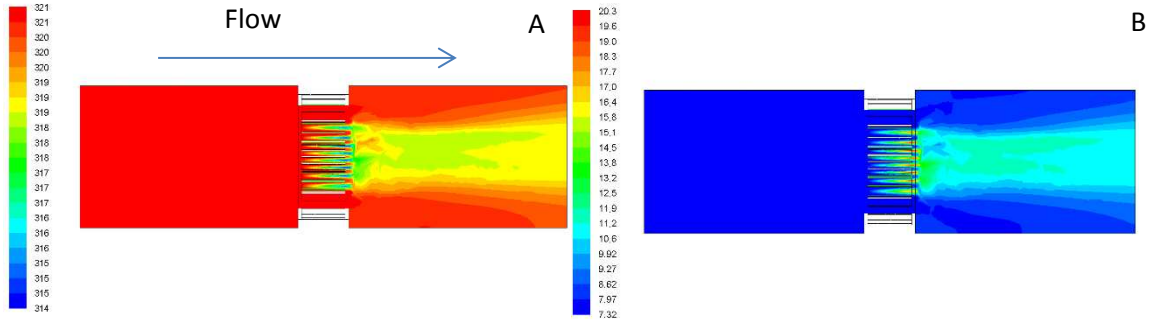

Figure 9 - Contours of a) temperature (in K) and b) relative humidity (%) for the CFD model of the regeneration air channel

The contours all exhibit a similar flow pattern as defined by the change in colours of the contours. The change in characteristics of the air is most notable around the centre of the duct, this runs intuitive to the design of the desiccant rotary wheel, the silica gel is positioned most dominantly at the centre of the wheel and so will have the most effect on the air. Both cases follow the anticipated pattern for air condition when relating to air temperature and relative humidity changes. For the inlet air channel, as the relative humidity of the air decreases as a result of the adsorption of water onto the surface of the silica gel, the air temperature increases. The opposite is seen in the regeneration air channel. The air temperature decreases as the relative humidity of the air increases. The effect of the silica gel is less pronounced in the regeneration air compared to the inlet air, this can be seen from the smaller band of affected air in Figure 12 compared to Figure 11. This supports the measurements seen in the experiment where desorption was lower than adsorption.

Experimental measurements of relative humidity and air temperature were collected at four points before and after the new design of desiccant rotary wheel. Measurements were made before and after the wheel in both the inlet and regeneration air channels. This was to provide a clear difference between the condition of the air before moving through the desiccant wheel and the condition of the air after under adsorption and desorption conditions. The measurement of the relative humidity and temperature from the four probes positioned in the channels, averaged for each minute of the duration of the experiment, are shown in Table 4.

Table 4 – Summary of experimental results

	Inlet Air Channel				Regeneration Air Channel			
	Before Wheel		After Wheel		Before Wheel		After Wheel	
Time (s)	Humidity [%rH]	Temp. [°C]	Humidity [%rH]	Temp. [°C]	Humidity [%rH]	Temp. [°C]	Humidity [%rH]	Temp. [°C]
0	41.70	26.70	26.20	28.10	7.10	47.90	10.20	44.60
60	42.33	26.57	26.05	28.09	7.04	47.98	10.26	44.14
120	42.02	26.00	26.51	28.66	6.80	48.79	10.64	44.37
180	79.77	23.48	29.45	29.20	6.70	49.03	10.83	44.28
240	81.78	22.45	29.15	29.65	6.70	48.91	10.83	44.32
300	82.47	21.92	28.49	29.83	6.90	48.38	11.21	43.82
360	83.43	21.37	27.84	30.00	7.10	47.88	11.26	43.46
420	89.13	20.80	27.65	30.11	7.20	47.70	11.51	43.35
480	93.35	20.40	27.82	30.00	7.10	48.00	11.66	43.59
540	93.54	20.33	28.71	30.09	6.81	48.83	10.71	44.69
600	91.28	20.11	27.46	30.37	6.60	49.68	10.23	45.29

From analysis of the values in the table, a number of conclusions can be drawn about the ability of the desiccant rotary to transfer moisture from one channel to the other. Additional humidity was not added to the inlet airstream for the initial two minutes of the experiment, this was done to provide a clear distinction between the condition of the air within the room and the inlet air at high relative humidity levels. For the first two minutes of activity, a decrease of approximately 16% relative humidity in the inlet air channel is seen, correlating to a 1.4-2.6°C increase in air temperature. This indicates a baseline level of moisture transport at low levels of inlet relative humidity. For the same time period, the regeneration shows an increase in relative humidity. The regeneration air temperature before the wheel of 47.9°C results in desorption of the silica gel particles and an increase in relative humidity in the regeneration air after the desiccant rotary wheel between 3.1-3.8%. The increase in relative humidity in this airstreams results in a reduced air temperature between 3.3-4.4°C.

The effect of the humidifier is seen from 180 seconds onwards as the relative humidity of the air increases up to a maximum of 93.54% after 540 seconds. Adsorption of the moisture increases at a linear rate as the relative humidity increases. This is clear as the relative humidity of the inlet air remains at a consistent level, similar to that seen prior to the introduction of the humidifier to the airstream. As the relative humidity of the inlet airstream after the wheel remains at a similar level for all relative humidity values before the wheel, predictions to the cause of this effect can be made. Due to the large volumes of open area in the desiccant rotary wheel, large volumes of air maybe unaffected by the silica gel. As the humidity probe measurements are taken as an average, the relative humidity of this air is diluted with the air that is affected by the silica gel. The degree of this effect is likely to be altered by the rotation velocity of the desiccant rotary wheel. A wheel rotating at a lower velocity will have a lower contact time if the humid air is moving rapidly through the wheel, causing less adsorption of the overall air. The greatest decrease in relative humidity in the inlet channel was measured as 65.53% after 480 seconds, this corresponded to a 9.6°C increase in air temperature. However, this was not the maximum temperature change in the inlet airstream. The temperature increase continued to rise after the maximum moisture transfer at 480 seconds. The maximum air temperature change was 10.26°C after 600 seconds, corresponding to a 63.82% decrease in relative humidity.

The disparity between the maximum relative humidity value, the maximum relative humidity change and the maximum temperature change in the inlet airstream is unexpected but can be explained. The maximum relative humidity value, measured at 540 seconds, is marginally higher than the relative humidity measured at 480 seconds when the maximum relative humidity change is measured. That the maximum change occurs at the time step before the maximum value is measured suggests that the silica gel particle may have become saturated and are no longer able to adsorb a greater volume of moisture. This provides a possible explanation between the discrepancy of the time step where the maximum relative humidity is measured and the maximum change. The maximum air temperature change is measured at the final experiment time step, when the probe will have experienced the maximum exposure time to the airstream, continually increasing the temperature of the probe. This is an important consideration as the probe uses a metallic hotwire to measure the air temperature. Continued exposure to the increasing air temperature will result in a lag time in the hotwire when a lower air temperature is introduced.

The change in relative humidity in the regeneration air channel reaches a peak value of 4.56%, also at 480 seconds. This suggests that as the maximum adsorption levels are reached by the silica gel particles, the maximum desorption rate is also experienced. This is as expected as the silica gel particles contain the highest volume of water available to be desorbed. The greatest air temperature change between the two measurement locations is at 180 seconds, the time when the effect of the introduction of the humidifier can be most clearly seen. The maximum air temperature reduction of 4.75°C at 180 seconds decreases to a minimum value of 4.14°C at 540 seconds. Though potentially surprising, this does follow the precedent shown in earlier results. The air temperature change at 540 seconds corresponds to a 3.90% increase in relative humidity. Earlier in the test, at 120 seconds, a 3.84% increase in relative humidity corresponded to a 4.42°C decrease in air temperature. This shows that though the values of relative humidity increase and air temperature decrease are correlated, they are not a predictable pattern. Two separate instances of equal relative humidity change result in different air temperature increase, 180 seconds and 240 seconds both show a 4.13% increase in relative humidity but a 4.75°C and 4.59°C decrease in air temperature respectively. At both 300 and 400 seconds, a 4.31% increase in relative humidity is measured but a 4.56°C and 4.35°C decrease in air temperature respectively. The difference between the two temperature decrease values is small, and so it is worth considering the accuracy of the measurement equipment as a cause of the apparent anomalies.

It is important to note that the regeneration air temperature, used for desorption of the water molecules from the silica gel particles, before the desiccant rotary wheel was 48.5°C. This represents a significant reduction in the regeneration air temperature previously used for desorption in rotary desiccant wheels. The regeneration air temperature is achieved by increasing the temperature of low-grade waste air, typically exhaust air from mechanical processes, using electric heaters. This has high energy costs by increasing the air temperature to 80-120°C. By showing that desorption can be achieved at significantly lower regeneration temperatures, the associated energy costs can be lowered or removed from the dehumidification process. This enhances the prospect of the desiccant rotary wheel with radial blades configuration.

Figure 10 shows the correlations between relative humidity and air temperature change before and after the desiccant rotary wheel in both the inlet and regeneration airstreams. The correlation between the relative humidity and air temperature change in the inlet air is 0.96 compared to 0.64

for the regeneration air. This shows that the influence of one of the factors on the other is significantly greater in the inlet air than the regeneration air.

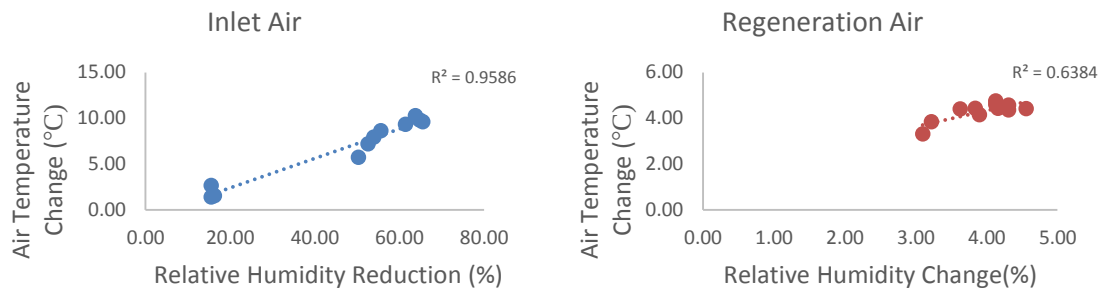

Figure 10 – Correlation between Humidity Change and Air Temperature Change in a) Inlet Air and b) Regeneration Air

The increased correlation in the inlet air compared to the regeneration air is likely due to a combination of reasons. The changes in relative humidity and air temperature measured in the regeneration air are generally of a lower value than the changes measured in the inlet air. Therefore, errors and deviation from the mean seen in the regeneration air have a greater effect in reducing the correlation of relative humidity and air temperature change.

Pressure Drop across Desiccant Rotary Wheel

In addition to the changes in air temperature and relative humidity affected by the new design of the desiccant rotary wheel, the pressure drop measured before and after the wheel is of importance. As current desiccant rotary wheels exhibit a high pressure drop in the air flow, the integration of these devices into ventilation systems requires additional equipment to circulate air and are unsuitable for natural ventilation systems. Minimising the pressure drop with the new design of the desiccant rotary wheel is a key characteristic of the potential of the device. Contours from the CFD analysis of the design showing the static pressure of the air in the channel can be seen below in Figure 11.

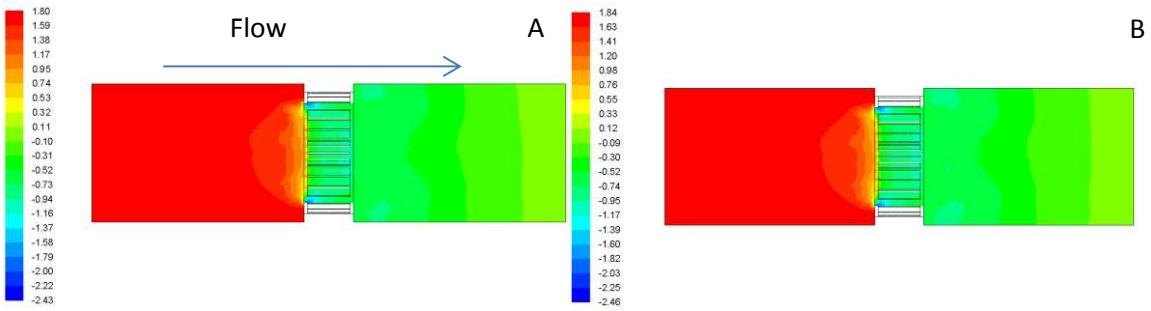

Figure 11 – CFD Contours of static pressure (Pa) a) inlet air channel and b) regeneration air channel

Measurements taken from the CFD models of the adsorption and desorption tests show that low pressure drop across the device is achieved. A pressure drop of 2.06Pa and 2.10Pa was measured for the adsorption and desorption tests respectively. The difference in the pressure drop between the two tests despite matching geometry is assumed to be due to the different air temperature of each of the tests. The low pressure drop measured for each test is encouraging for the development of the device. A low pressure drop suggests that integration into natural ventilation systems is possible and mechanical ventilation systems would not require additional equipment for supply air.

The goal of limiting the pressure drop is to ensure that the velocity of the air moving through the desiccant rotary wheel, particularly in the inlet air channel, remains high enough to provide adequate air supply rates for possible integration into passive ventilation systems. To do this, a pressure drop no greater than 2Pa was viewed as acceptable. Because of the low air velocities of passive ventilation systems, a pressure drop greater than this would result in very low air supply rates, this has been confirmed in early work on passive ventilation systems [45].

Equation 1

$$p_1 + \frac{1}{2}\rho {V_1}^2 + \rho g h = p_2 + \frac{1}{2}\rho {V_2}^2 + \rho g h$$

It can be seen from studying the Bernoulli Equation in Equation 1, that the balance between pressure and velocity before the wheel and after the wheel must be maintained for a fluid. As can be seen in Figure 11, the pressure before the wheel is higher than the pressure after the wheel in both cases. Because of the reduction in pressure, air velocity after the wheel must increase to provide balance to the Bernoulli Equation. It was shown in the CFD analysis that the velocity before the wheel was 0.85m/s for both conditions and 1.65m/s and 1.64m/s for the adsorption and desorption respectively. This remains consistent with the Bernoulli Equation. The contraction of the air flow through the wheel will result in acceleration of the air as it passes through. The results further highlight the benefit of the new design for the rotary desiccant wheel in reducing pressure without affecting the air velocity, providing evidence for integration into passive ventilation systems with further investigation.

Only a single alternative design of matrix structure has been tested in this work, further work would seek to explore more designs. Increased/decreased number of blades, optimised size of blades and the silica gel particles, alternative matrix designs in a concentric circle or similar arrangement, a range of inlet/regeneration air temperatures, relative humidity and air velocities can all be tested to improve the experimental testing.

Conclusion

The ability of a new design of desiccant rotary wheel with 28 silica gel coated radial blades to reduce the relative humidity of an airstream and the pressure drop across the wheel was tested experimentally using a prototype setup and validated a CFD simulation. Adsorption of moisture in the inlet airstream up to 65% was noted whilst increasing the air temperature of the inlet air by 9.6°C. Furthermore, constant regeneration of the desiccant material was achieved at a regeneration temperature of 48.5°C, significantly lower than regeneration temperatures commonly used in desiccant systems. The pressure drop across the desiccant rotary wheel was measured as 2.06Pa, lower than the pressure drop across the matrix of traditional desiccant rotary wheel designs.

The results from the CFD analysis and experiments show that the new design of the desiccant rotary wheel has many potentials that could help to significantly improve the condition of incoming air, as well as reduce energy demand for building operators. The proposed arrangement of silica gel particles on the surface of the blades show high adsorption of water from the air, which is able to be regenerated. Lowering the relative humidity of the air aids in the conditioning of air for improved thermal comfort to occupants. The regeneration temperature required is significantly lower than the

temperature previously used in desiccant systems. This provides some evidence that lower regeneration temperatures may be used for desorption of the silica gel and so provide a reduction in the total energy use of the system.

As this experiment ran for a comparatively short time, an estimation of the energy saved was not made. Prolonged running of the experiment would be beneficial to ensure that the operation of the wheel is suitable beyond a running time of 10 minutes. As operations of desiccant wheels can be up to 24 hours per day, it will be necessary to ensure if complete saturation of the silica gel particles is possible and if the continuous desorption process is adequate to prevent this situation. Full integration of the device into mechanical and natural ventilation systems would provide a useful comparison of air quality, supply rates and energy consumption, between each other and with existing systems.

As the pressure drop across the wheel has been reduced, the need for additional blowers and fans commonly used in mechanical systems are not required, it is likely that sufficient supply air can be generated. This further reduces the energy requirements of the system. As the pressure drop is approximately 2Pa, the integration of this device into natural ventilation systems is possible. These systems require no energy for ventilation, enhancing the low energy characteristics of the device.

The results of this work show that an alternative design of desiccant rotary wheels from the conventional honeycomb/sinusoidal wave structure is capable of reducing the relative humidity of an incoming airstream with a lower regeneration air temperature and a lower pressure drop experienced by the airstream. Despite the successes of the design, significant more areas of research and optimisation are required.

Acknowledgements

The authors of this paper would like to acknowledge the support of The University of Leeds Civil Engineering department and the support of The University of Sheffield Mechanical Engineering department. The work presented in this paper is covered by the UK patent GB1506768.9.

References

[1] A.M. Omer, Renewable building energy systems and passive human comfort solutions, Renew. Sustain. Energy Rev. 12 (2008) 1562–1587. doi:10.1016/j.rser.2006.07.010.

[2] R. Parameshwaran, S. Kalaiselvam, S. Harikrishnan, A. Elayaperumal, Sustainable thermal energy storage technologies for buildings : A review, Renew. Sustain. Energy Rev. 16 (2012) 2394–2433. doi:10.1016/j.rser.2012.01.058.

[3] Y. El Fouih, P. Stabat, P. Rivière, P. Hoang, V. Archambault, Adequacy of air-to-air heat recovery ventilation system applied in low energy buildings, Energy Build. 54 (2012) 29–39. doi:10.1016/j.enbuild.2012.08.008.

[4] A. Boyano, P. Hernandez, O. Wolf, Energy demands and potential savings in European office buildings: Case studies based on EnergyPlus simulations, Energy Build. 65 (2013) 19–28. doi:10.1016/j.enbuild.2013.05.039.

[5] J. Laverge, A. Janssens, Heat recovery ventilation operation traded off against natural and simple exhaust ventilation in Europe by primary energy factor, carbon dioxide emission, household consumer price and exergy, Energy Build. 50 (2012) 315–323.

doi:10.1016/j.enbuild.2012.04.005.

[6] L.Z. Zhang, D.S. Zhu, X.H. Deng, B. Hua, Thermodynamic modeling of a novel air dehumidification system, 37 (2005) 279–286. doi:10.1016/j.enbuild.2004.06.019.

[7] B. Givoni, Indoor temperature reduction by passive cooling systems, Sol. Energy. 85 (2011) 1692–1726. doi:10.1016/j.solener.2009.10.003.

[8] P. Mazzei, F. Minichiello, D. Palma, HVAC dehumidification systems for thermal comfort : a critical review, 25 (2005) 677–707. doi:10.1016/j.applthermaleng.2004.07.014.

[9] S.B. Riffat, M.C. Gillott, Performance of a novel mechanical ventilation heat recovery heat pump system, Appl. Therm. Eng. 22 (2002) 839–845.

[10] N.C.L. Brum, Modeling and simulation of heat and enthalpy recovery wheels, Energy. 34 (2009) 2063–2068. doi:10.1016/j.energy.2008.08.016.

[11] T.S. Ge, Y. Li, R.Z.Ã. Wang, Y.J. Dai, A review of the mathematical models for predicting rotary desiccant wheel, 12 (2008) 1485–1528. doi:10.1016/j.rser.2007.01.012.

[12] Y. Tashiro, M. Kubo, Y. Katsumi, T. Meguro, K. Komeya, Assessment of adsorption-desorption characteristics of adsorbents for adsorptive desiccant cooling system, J. Mater. Sci. 39 (2004) 1315–1319. doi:10.1023/B:JMSC.0000013937.11959.6a.

[13] C.X. Jia, Y.J. Dai, J.Y. Wu, R.Z. Wang, Experimental comparison of two honeycombed desiccant wheels fabricated with silica gel and composite desiccant material, Energy Convers. Manag. 47 (2006) 2523–2534. doi:10.1016/j.enconman.2005.10.034.

[14] J.L. Niu, L.Z. Zhang, Membrane-based Enthalpy Exchanger : material considerations and clarification of moisture resistance, J. Memb. Sci. 189 (2001) 179–191.

[15] G. Angrisani, F. Minichiello, C. Roselli, M. Sasso, Experimental analysis on the dehumidification and thermal performance of a desiccant wheel, Appl. Energy. 92 (2012) 563–572. doi:10.1016/j.apenergy.2011.11.071.

[16] J. Taweekun, V. Akvanich, The Experiment and Simulation of Solid Desiccant Dehumidification for Air-Conditioning System in a Tropical Humid Climate, Engineering. 2013 (2013) 146–153.

[17] A. Mardiana, S.B. Riffat, Review on physical and performance parameters of heat recovery systems for building applications, Renew. Sustain. Energy Rev. 28 (2013) 174–190. doi:10.1016/j.rser.2013.07.016.

[18] L.Z. Zhang, J.L. Niu, Performance comparisons of desiccant wheels for air dehumidification and enthalpy recovery, 22 (2002) 1347–1367.

[19] D.G. Waugaman, A. Kini, C.F. Kettleborough, A Review of Desiccant Cooling Systems, J. Energy Resour. Technol. 115 (1993) 1. doi:10.1115/1.2905965.

[20] C. Roulet, F.D. Heidt, F. Foradini, M. Pibiri, Real heat recovery with air handling units, 33 (2001) 495–502.

[21] G. Angrisani, C. Roselli, M. Sasso, Experimental assessment of the energy performance of a hybrid desiccant cooling system and comparison with other air-conditioning technologies, Appl. Energy. 138 (2015) 533–545. doi:10.1016/j.apenergy.2014.10.065.

[22] X.J. Zhang, Y.J. Dai, R.Z. Wang, A simulation study of heat and mass transfer in a

honeycombed rotary desiccant dehumidifier, 23 (2003) 989–1003. doi:10.1016/S1359-4311(03)00047-4.

[23] N. Enteria, H. Yoshino, A. Satake, A. Mochida, R. Takaki, R. Yoshie, et al., Experimental heat and mass transfer of the separated and coupled rotating desiccant wheel and heat wheel, Exp. Therm. Fluid Sci. 34 (2010) 603–615. doi:10.1016/j.expthermflusci.2009.12.001.

[24] Y. Fan, K. Ito, Energy consumption analysis intended for real office space with energy recovery ventilator by integrating BES and CFD approaches, Build. Environ. 52 (2012) 57–67. doi:10.1016/j.buildenv.2011.12.008.

[25] M. Intini, S. De Antonellis, C.M. Joppolo, The effect of inlet velocity and unbalanced flows on optimal working conditions of silica gel desiccant wheels, Energy Procedia. 48 (2014) 858–864. doi:10.1016/j.egypro.2014.02.099.

[26] K. Keniar, K. Ghali, N. Ghaddar, Study of solar regenerated membrane desiccant system to control humidity and decrease energy consumption in office spaces, Appl. Energy. 138 (2015) 121–132. doi:10.1016/j.apenergy.2014.10.071.

[27] B.R. Hughes, J.K. Calautit, S.A. Ghani, The development of commercial wind towers for natural ventilation: A review, Appl. Energy. 92 (2012) 606–627. doi:10.1016/j.apenergy.2011.11.066.

[28] B.R. Hughes, C.M. Mak, A study of wind and buoyancy driven flows through commercial wind towers, Energy Build. 43 (2011) 1784–1791. doi:10.1016/j.enbuild.2011.03.022.

[29] D. Mumovic, J. Palmer, M. Davies, M. Orme, I. Ridley, T. Oreszczyn, et al., Winter indoor air quality, thermal comfort and acoustic performance of newly built secondary schools in England, Build. Environ. 44 (2009) 1466–1477. doi:10.1016/j.buildenv.2008.06.014.

[30] M. Kolokotroni, B.C. Webb, S.D. Hayes, Summer cooling with night ventilation for office buildings in moderate climates, Energy Build. 27 (1998) 231–237. doi:10.1016/S0378-7788(97)00048-0.

[31] D.J. Clements-Croome, H.B. Awbi, Z. Bak??-Bir??, N. Kochhar, M. Williams, Ventilation rates in schools, Build. Environ. 43 (2008) 362–367. doi:10.1016/j.buildenv.2006.03.018.

[32] A.W. Woods, S. Fitzgerald, S. Livermore, A comparison of winter pre-heating requirements for natural displacement and natural mixing ventilation, Energy Build. 41 (2009) 1306–1312. doi:10.1016/j.enbuild.2009.07.030.

[33] Health and Safety Executive, Workplace health, safety and welfare, (2013) 19.

[34] D. O'Connor, J.K. Calautit, B.R. Hughes, A study of passive ventilation integrated with heat recovery, Energy Build. 82 (2014) 799–811. doi:10.1016/j.enbuild.2014.05.050.

[35] A. Mardiana, S.B. Riffat, M. Worall, Integrated heat recovery system with wind-catcher for building applications : towards energy-efficient technologies, Mater. Process. Energy Commun. Curr. Res. Tech. Dev. (2013) 720–727.

[36] J.K. Calautit, H.N. Chaudhry, B.R. Hughes, S.A. Ghani, Comparison between evaporative cooling and a heat pipe assisted thermal loop for a commercial wind tower in hot and dry climatic conditions, Appl. Energy. 101 (2013) 740–755. doi:10.1016/j.apenergy.2012.07.034.

[37] S. Soutullo, C. Sanjuan, M.R. Heras, Energy performance evaluation of an evaporative wind

tower, Sol. Energy. 86 (2012) 1396–1410. doi:10.1016/j.solener.2012.02.001.

[38] P. Bourdoukan, E. Wurtz, P. Joubert, M. Spe, Potential of solar heat pipe vacuum collectors in the desiccant cooling process : Modelling and experimental results, 82 (2008) 1209–1219. doi:10.1016/j.solener.2008.06.003.

[39] N. Enteria, H. Yoshino, A. Mochida, R. Takaki, A. Satake, Construction and initial operation of the combined solar thermal and electric desiccant cooling system, Sol. Energy. 83 (2009) 1300–1311. doi:10.1016/j.solener.2009.03.008.

[40] J. Jeong, S. Yamaguchi, K. Saito, S. Kawai, Performance analysis of four-partition desiccant wheel and hybrid dehumidification air-conditioning system ´ shydratante a ` quatre Analyse de la performance d ' une roue de ` me de conditionnement d ' air a segments et d ' un syste ´ shydratant hybride d, Int. J. Refrig. 33 (2010) 496–509. doi:10.1016/j.ijrefrig.2009.12.001.

[41] L.Z. Zhang, Energy performance of independent air dehumidification systems with energy recovery measures, Energy. 31 (2006) 1228–1242. doi:10.1016/j.energy.2005.05.027.

[42] J.K. Calautit, H.N. Chaudhry, B.R. Hughes, L. Sim, A validated design methodology for a closed-loop subsonic wind tunnel, Jnl. Wind Eng. Ind. Aerodyn. 125 (2014) 180–194. doi:10.1016/j.jweia.2013.12.010.

[43] B.R. Hughes, S.A.A.A. Ghani, A numerical investigation into the effect of Windvent louvre external angle on passive stack ventilation performance, Build. Environ. 45 (2010) 1025–1036. doi:10.1016/j.buildenv.2009.10.010.

[44] ANSYS, ANSYS Fluent Theory Guide, (2013) 814.

[45] L. Shao, S.B. Riffat, G. Gan, Heat recovery with low pressure loss for natural veltilation, Energy Build. 28 (1998) 179–184. doi:10.1016/S0378-7788(98)00016-4.